Flow Investigation In A Francis Draft Tube : The Flindt Project

François Avellan
EPFL - Laboratory for Hydraulic Machines, Lausanne, Switzerland

ABSTRACT

The flow investigation in a elbow draft tube is presented. After a review of the existing works related to the flow analysis of such component, the need of an experimental validation of the CFD tools is discussed with respect the practical interest of improving the matching of a runner and the draft tube. The geometry and the main characteristics of the test model is described and the pressure recovery coefficient is provided in an extended operating range. The instrumentation of the draft tube and the LDA system for flow survey are described. After the discussion of the influence of the boundary conditions and the mesh size with respect to the CFD analysis, the results of flow analysis are compared to the available experimental data for 3 operating points.

RESUME

L'étude de l'écoulement dans un diffuseur coudé est présentée. Après une revue des travaux existants sur l'analyse d'écoulement dans ce type de composant, on met en évidence le besoin d'une validation expérimentale des logiciels de calcul d'écoulements en vue de l'intérêt pratique d'améliorer l'adaptation d'une roue au diffuseur. La géométrie et les caractéristiques principales du model d'essai sont décrites et le coefficient de récupération de pression fourni pour un domaine de fonctionnement étendu de la turbine. L'instrumentation du diffuseur ainsi que le système de sondage d'écoulement par LDA sont détaillés. Après une discussion de l'influence des conditions aux limites et de la taille du maillage, les résultats de calculs d'écoulements sont comparés aux mesures disponibles pour 3 points de fonctionnement.

NOMENCLATURE

Term	Symbol	Definition	Term	Symbol	Definition
Cross Section Area	A		Number of rpm	N	
Flow Velocity	C		Angular Speed	ω	
Turbulent Velocity	c'		Specific speed	ν	$\omega\sqrt{Q/\pi}/(2E$
Runner Diameter	D		Unit Specific speed	n_q	$N\sqrt{Q}/H^{3/4}$
Specific Hydraulic Energy	E	gH	Discharge	Q	
Energy Coefficient	ψ	$2E/(\omega D/2)^2$	Discharge Coefficient	φ	$Q/\pi\omega(D/2)^3$
Kinetic Energy Factor	φ^2/ψ	$Q^2/\pi^2(D/2)^4$	Discharge Factor	Q_{ED}	$Q/D^2\sqrt{E}$
Gravity Acceleration	g		Unit Discharge	Q_{11}	$Q/D^2\sqrt{H}$
Net Head	H		Efficiency	η	
Specific Turbulent Kinetic Energy	k	$\sum\overline{c'^2_i}/2$	Pressure Recovery Coefficient	χ	
Net Specific Positive Energy	$NPSE$		Dynamic Viscosity	μ	
Thoma Number	σ	$NPSE/E$	Best Efficiency Point	BEP	
Water density	ρ		Inlet Section of the Draft Tube	REF	

INTRODUCTION

The draft tube of an hydraulic turbine is the machine component where the flow exiting the runner is decelerated, thereby converting the excess of kinetic energy into static pressure. Therefore, the specific pressure energy recovery in the draft tube affects significantly the efficiency and power output of machines with a high discharge factor, Q_{ED}. The flow analysis of this component is then of practical interests for either the design of new machines or the rehabilitation of existing ones. Thus, it is not surprising that numerous studies related to the computation of the flow in hydraulic turbine draft tubes have been reported during the last decades, however there are only few which include experimental validation of the numerical results. We can report the work of T. C. Vu & W. Shyy in1988, (Ref. 1) which compare the results of viscous flow analysis with detailed air experimental data, the draft tube being installed in a wind tunnel. In 1990, Tanabe et al. (Ref. 2), Combes et al. (Ref. 3) and Ruprecht (Ref. 4) reported comparisons between turbulent flow analysis and measurements with a rather good agreement in case of modern design of draft tubes. In 1994, Ruprecht et al. (Ref. 5) provided more detailed comparisons of CFD with experimental results obtained by Laser Doppler Anemometry with a fixed swirl generator, Parkinson et al. (Ref. 6) reported also good partial comparisons between CFD and experimental flow surveys obtained with a 5 holes pressure probe at the outlet of a draft tube of a Francis Turbine Model. In 1996, Ventikos et al. (Ref. 7) could report the experimental validation of a near wall turbulence closure scheme for the case of the draft tubes of the Norris power plant.

However, despite the excellent quality of the studies described in the above mentioned references, we can observe that there is still a need for comparison and validation of CFD results with respect to the detailed measurements of the velocity, the pressure fields or the turbulent characteristics of the flow. Nevertheless, the lack of measurement data did not prevent the manufacturers from developing a modern CFD practice for the design and/or the improvement of elbow draft-tubes and it could be acknowledged that they are successful in achieving a good peak efficiency. Today CFD as a design and analysis tool is applied routinely to all the component of the machine, see for instance Keck et al. (Ref. 8).

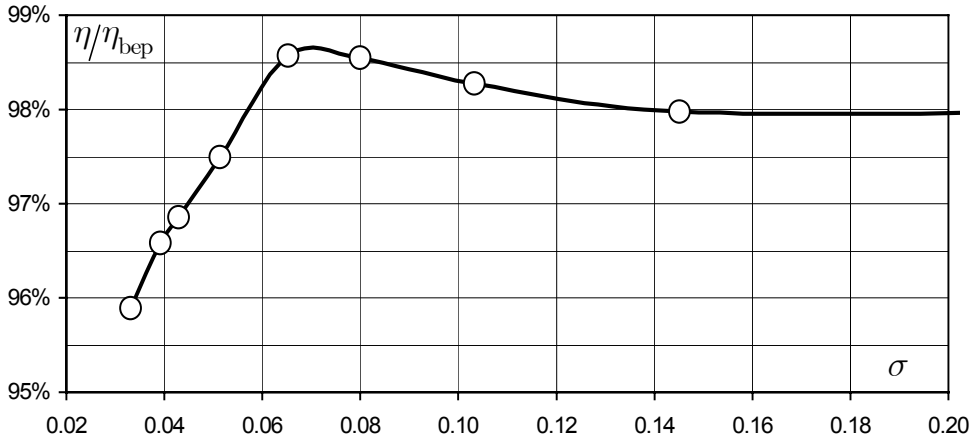

Figure 1 Cavitation curve of a model of a $\nu = 0.4$ ($n_q = 84$) Francis Turbine

However, it is still challenging to determine the optimum flow distribution at the runner outlet which leads to the best overall performance of the machine including efficiency, power output and smooth regime for an extended operating range. Simply let us consider, during model

testing, the influence of the Thoma number on the efficiency which often shows an increase with the development of the cavity rope, see Figure 1. This efficiency increase can be considered as a measure of the potential gain in the improvement of the matching of the runner with the draft tube. Moreover, for any attempt to minimize the pressure fluctuations level of a new Francis turbine design, it would be a prerequisite to understand the influence on these pressure fluctuations level of flow in the draft tube.

In the case of machine rehabilitation of an existing power plant, mostly only the runner and the guide vanes are currently modified. For economical and safety reasons, the spiral casing and the draft tube are seldom redesigned, however the installation of a redesigned runner absolutely needs to predict the flow in the draft tube in order to overcome the unexpected efficiency curve illustrated Figure 2. In the case of the rehabilitation of this machine, the measured efficiency for the existing runner shows that the upgraded runner leads to an increase of both the peak efficiency, 1 %, and the corresponding discharge value, 10 %. However for this machine, a sudden 1.2% drop of the efficiency is observed by increasing the discharge, the specific kinetic energy at the runner outlet being 11 % of the machine specific energy, $Q_{ED} = 0.367$ ($Q_{11} = 1.149$). Moreover, the efficiency shows a hysteresis when the discharge is decreased.

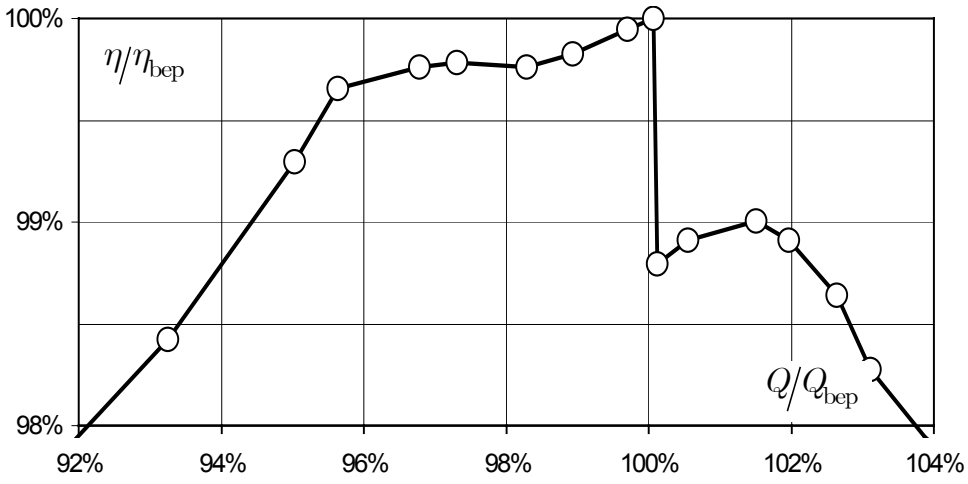

Figure 2 Efficiency break off obtained by increasing the discharge and keeping the specific energy constant, model test of the upgraded runner of a $\nu = 0.6$ ($n_q = 93$) Francis Turbine

This type of behavior which was reported, for instance, by Nichtawitz and Abfalterer for the case of a Kaplan Turbine, Figure 7 of Ref. 9, is strongly dependent on the draft tube cross section area law, see Figure 3, and the corresponding flow phenomena are very complex.

Depending on the machine operating point the incoming flow rotation is superposed to a highly turbulent non-uniform flow, subjected to separation swirls and transient phenomena in the elbow and the diffusing exit. When the incoming swirl intensity is not high enough, the flow is suddenly unbalanced and a part of the draft tube flow is completely separated and often a strong back-flow from the tail race channel can also be observed.

Considering the complex characteristics of the flow in a elbow draft tube, the need for an extensive experimental validation of the CFD tools arises among the community involved in the rehabilitation of hydropower plants. The practical importance of predicting these complex flow regimes leads to build up the FLINDT research project of Flow Investigation in Draft

Tubes within EUREKA, the pan-European framework for research and development cooperation, (Ref. 10). Therefore the objective of the project is to investigate the flow in hydraulic turbines draft tubes for a better understanding of the physics of these flows and to build up an extensive experimental data base describing a wide range of operating points which can provide a firm basis for the assessment of the CFD engineering practice in this component. With respect to these objective, the following issues are in particular addressed:

- analysis of specific energy losses (vorticity generation, turbulence influence, unsteady effects, ...) for physical understanding and modeling and for improving the prediction techniques of draft tube efficiency ;
- understanding of the draft tube flow behavior corresponding to the break off of the efficiency while increasing the discharge as in Figure 2;
- influence of flow instabilities on vibratory behavior;
- control of the flow mixing in the draft tube and its possible impact on the aeration of the tail water channel.

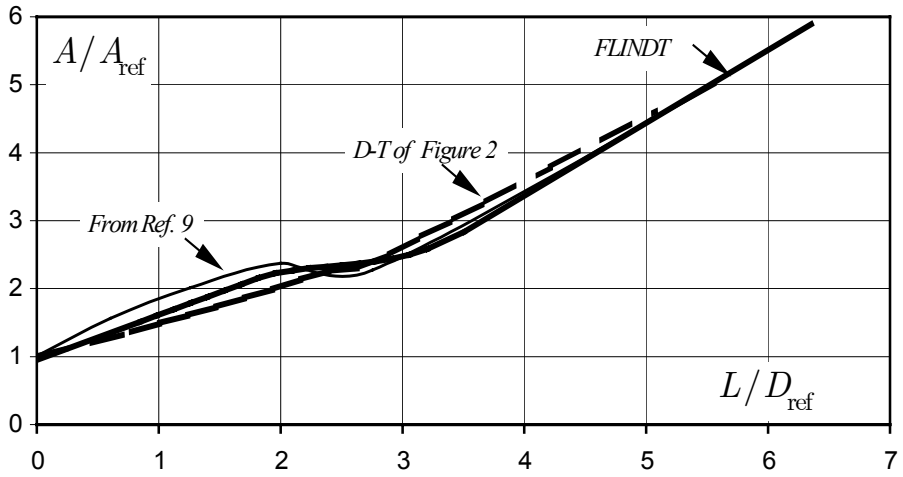

Figure 3 Cross section area laws for the FLINDT draft tube and the draft tubes from Ref. 9 and Figure 2 respectively.

The present paper intends to present a general view of the studies carried out within the FLINDT project by detailing the model test case, the specific instrumentation suited for the concern of the flow analysis in this component and finally the comparisons of CFD and experimental results. The Francis turbine model is first introduced and the geometry of the draft tube described. Then, the instrumentation used for the flow investigation in the draft tube is described. For practical cases, however, the engineer usually has very little information on the inlet boundary conditions. This study give indications on the influence of parameters that must be introduced for a computation with a standard approach, therefore the influence of the turbulent dissipation rate inlet condition is discussed as also the mesh quality and the outlet boundary conditions. Moreover it should be noticed that this paper focuses on the modeling and therefore an interpretation of the flow behavior in the draft tube is not attempted here.

MODEL TESTS

The investigated model is a Francis turbine of high specific speed, $\nu = 0.56$, ($n_q = 88$) corresponding to the machines of a 1926 old hydropower plant owned by ALCAN. The 4.1 m diameter runners of the machines were upgraded in the late 80. However the draft tubes of

these machines are of the Moody type, so an elbow draft tube was especially designed for the purpose of the project.

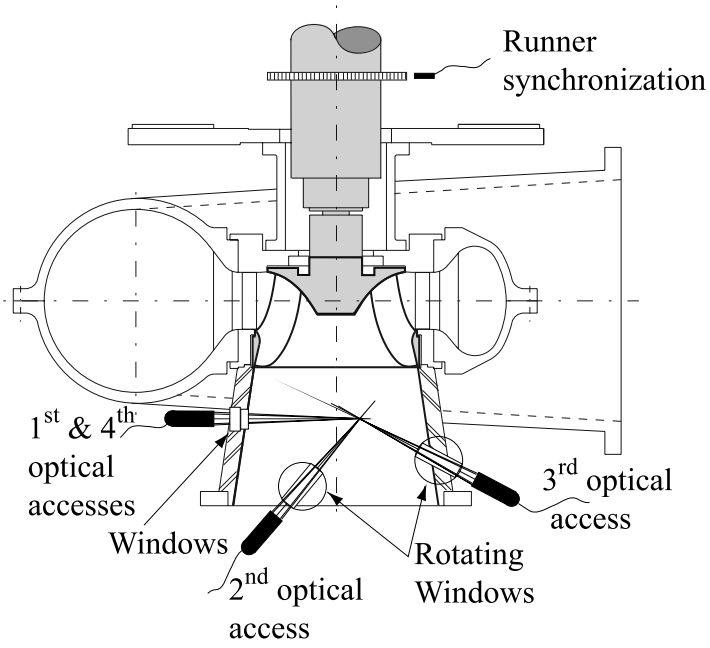

Figure 4 Francis Turbine Model and LDA paths for the flow survey in the draft tube cone

The main characteristics of the model are, see Figure 4:

- a spiral casing of double curvature type with a stay ring of 10 stay vanes;
- a distributor made of 20 guide vanes;
- a 17 blades runner of a 0.4 m outlet diameter;
- a symmetric elbow draft tube with 1 pier substituted to the original Moody draft tube.

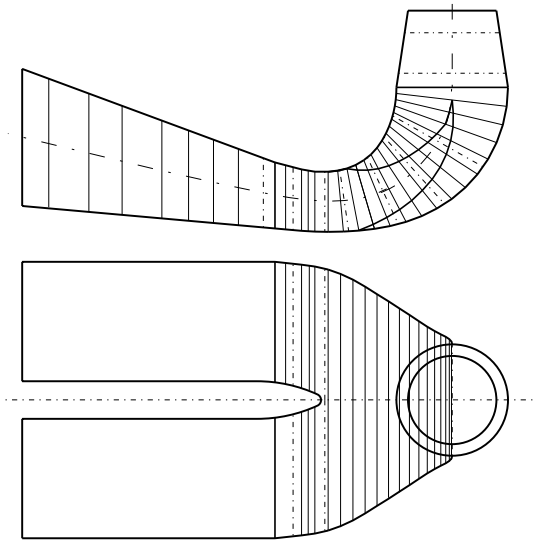

Figure 5 Side and top views of the FLINDT draft tube

The geometry of the draft tube is carefully selected in order to obtain the desired efficiency break-off with the discharge, see Figure 6. The short conical diffuser of 8° half angle is

followed by a 90° curved elbow and, then, by a rectangular section diffuser with 1 pier see Figure 5 and Figure 3 for the cross section area law.

The global measurements of flow, head and efficiency are performed according to the IEC standards (Ref. 11) at the Laboratory for Hydraulic Machines of EPFL.

The specific kinetic energy of the flow at the outlet of the runner represents 12.2 % of the model specific energy at the best efficiency point, $Q_{ED} = 0.391$ ($Q_{11} = 1.224$).

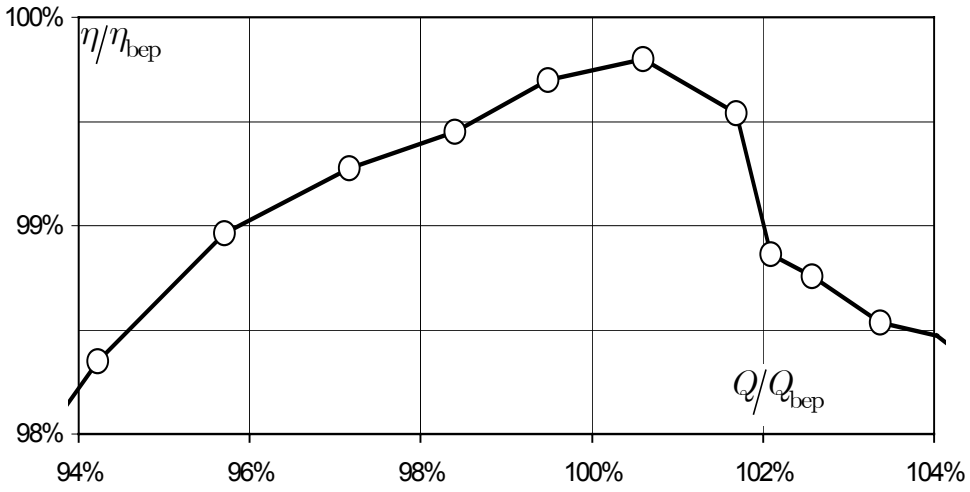

Figure 6 Efficiency break off obtained by increasing the discharge and keeping the specific energy constant, Flindt model with the final draft tube version

A global behavior of the draft tube can be investigating by introducing χ the static pressure recovery coefficient, (Ref. 9), which can be simply derived from the discharge and the measurement of the difference of the mean wall pressure between the inlet and the outlet sections of the draft tube according to the following relation:

$$\chi = \frac{\left(p/\rho + gZ_2\right) - \left(p_{ref}/\rho + gZ_{ref}\right)}{\left(1 - A_2^2/A_{ref}^2\right)Q^2/2A_{ref}^2} \approx \frac{\left(p/\rho + gZ_2\right) - \left(p_{ref}/\rho + gZ_{ref}\right)}{Q^2/2A_{ref}^2}$$

It should be noticed that the mean specific kinetic energy at the draft tube outlet can be neglected as compared to the specific kinetic energy at the draft tube inlet.

The corresponding values of the pressure recovery coefficient are given for the different operating conditions of the machine Figure 7. As it could be expected, the break off of the pressure recovery is strongly influenced by the discharge coefficient, the specific energy coefficient influence being sensitive for the high values of ψ, the specific energy coefficient. By varying the test head, one could check that the Reynolds number does not have any visible influence on the pressure recovery coefficient.

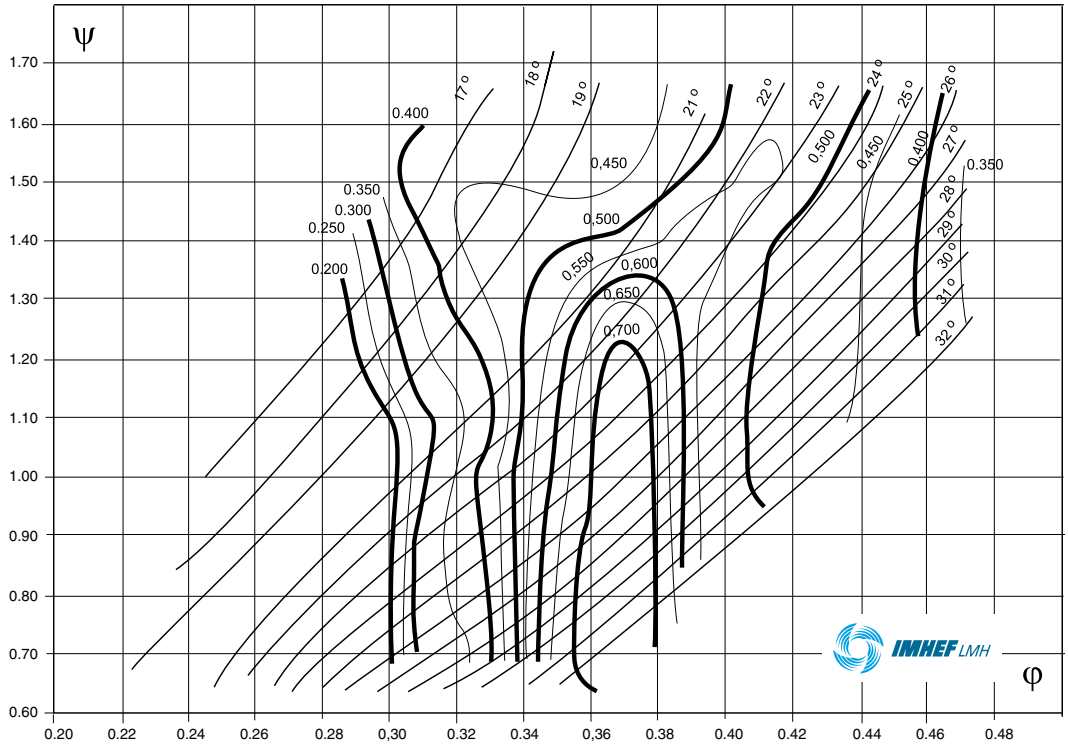

Figure 7 Hill chart of χ, the static pressure recovery coefficient

MEASUREMENT SYSTEMS

The measurement systems are specified in order to provide to the computational flow analysis the required boundary conditions and several flow field values at given reference sections for validation purpose. Moreover, the unsteadiness characteristics of the flow should be investigated since unsteady computations are envisioned. Thus, the draft tube is equipped with a transparent cone and with optical windows, see Figure 8 for the flow survey with the help of the LDA. The optical windows can be removed and plates equipped with miniature piezo resistive pressure transducers can be put in place. 42 piezo resistive pressure transducers are also embedded see Figure 8 in the inlet edge of the pier.

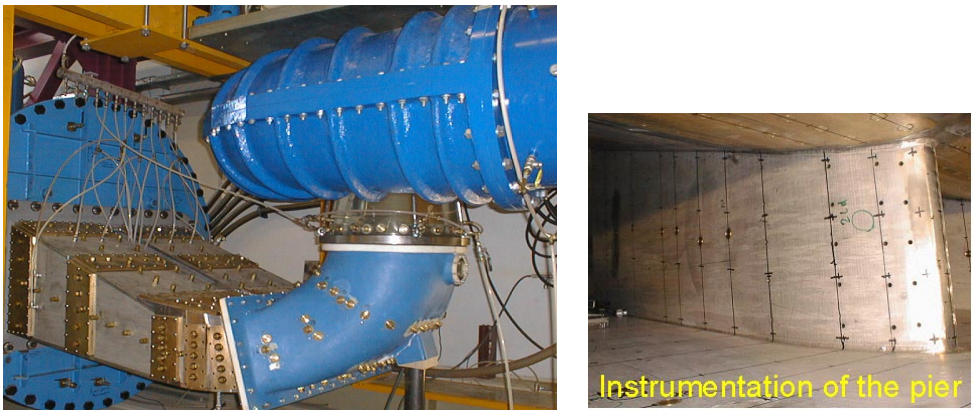

Figure 8 Draft Tube Instrumentation

The pressure transducer embedding technology is the same as the one described in Ref. 14. Up to 96 pressure taps can be acquired simultaneously at a maximum sampling rate of

50 kHz. Synchronization of the pressure signals with the runner angular position is carried out with a help of an 9'000 pulses optical encoder mounted on the runner shaft, see Figure 4.

Five holes pressure probes are used to perform a full traversing steady flow survey in any section of interest of the draft tube. The probe is mounted on a specific 2 axes remote traversing system support of which both the relative linear and the angular positions are given by optical encoders, Figure 9. The local static pressure and the 3 components of the mean flow velocity are derived from the 5 pressure readings accordingly to the procedure described by Avellan et al. (Ref. 13). All the geometrical coordinates of both the pressure taps or the flow survey paths are defined inside the CATIA® CAD model of the FLINDT draft tube.

Figure 9 Five holes pressure probe mounted on the 2 axes remote traversing system

The Laser Doppler Anometer LDA is a Dantec® 2 components probe, using back-scattered light and transmission by optical fiber, with a laser of 5W Argon-ion source. The main characteristics of the optical system are presented Table 1.

Characteristics	
Laser wave lengths	488 / 514.5 nm
Probe diameter	60 mm
Beam expander	112 mm
Beam spacing probe with beam expander	38 mm 73.3 mm
Focal length	400/600/1000 mm
Fringe spacing	~5.3 nm
Measuring volume	$\sigma_x=\sigma_y$ ~0.12 / 0.2 mm σ_z ~2.34 / 6 mm

Table 1 Optical characteristics of the laser probes

Spherical silver coated hollowed glass particles of 10 μm diameter are seeded in the test rig circuit to improve the data sampling rate. For the flow survey the LDA Probe is installed on a mounting bench, see Figure 10.

In order to obtain the 3D components of the flow velocity with a 2D laser probe, non-orthogonal optical arrangements are used in the cone, Figure 4. Two components are obtained by a direct measurement - the first optical access. The third component is obtained with the second optical access; a rotating window is used to measure two other components of the velocity vector. The accuracy of the measurement volume position is of the same magnitude that σ_Z dimensions, see Table 1.

The LDA signal bursts are also synchronized with the runner angular position with the help of the optical encoder mounted on the runner shaft.

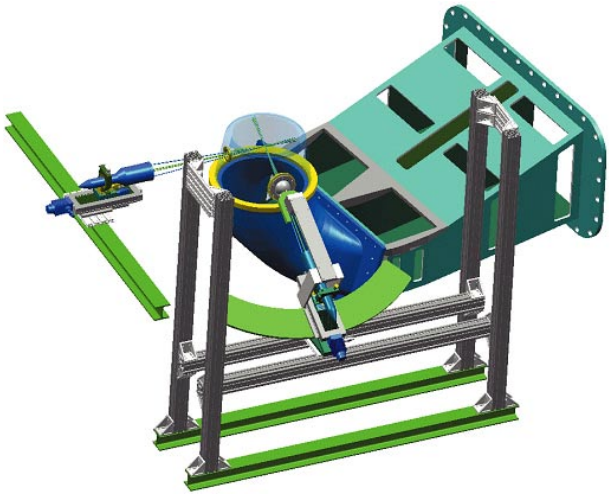

Figure 10 Mounting bench of the LDA for the flow survey in the draft tube cone

The synchronized signal allows us to apply the phase averaging technique to the LDA bursts in order to extract the periodic component of the flow velocity. An example of such periodic flow field is given Figure 11. For the lower discharge coefficient before the pressure recovery break off takes place the respective wake of the 17 runner blades is well visible with a positive rotation of the flow which extends to the core region. For the higher discharge coefficient, beyond the χ break off, the wakes are more diffused and the flow rotation is reduced as it could be expected.

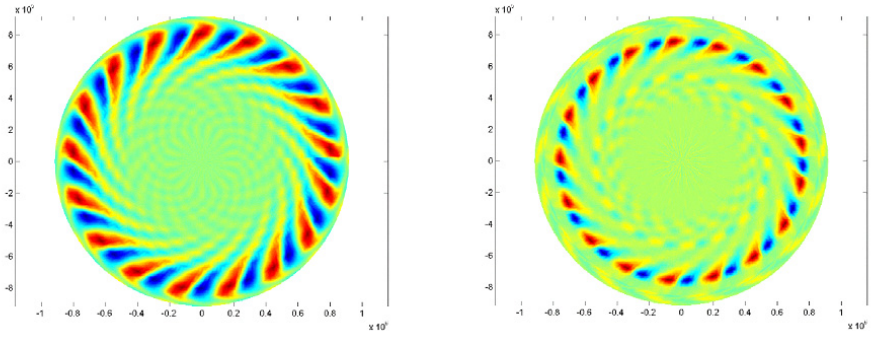

$\varphi = 0.350$ $\varphi = 0.390$

Figure 11 Periodic velocity field at the inlet section of the draft tube for both low and high discharge coefficient operating points

The availability of 4 different optical accesses lead to the derivation of the 6 components of the turbulent stress tensor through an appropriate geometrical transform, see Ciocan et al. (Ref. 12). The distribution of the mean values of these components along the radial position at the inlet section A_{ref} are given for 2 operating points from each side where the break off takes place. It can be observed that the highest values of turbulent stresses take place in the core region where the diffusion of the blade wakes is observed.

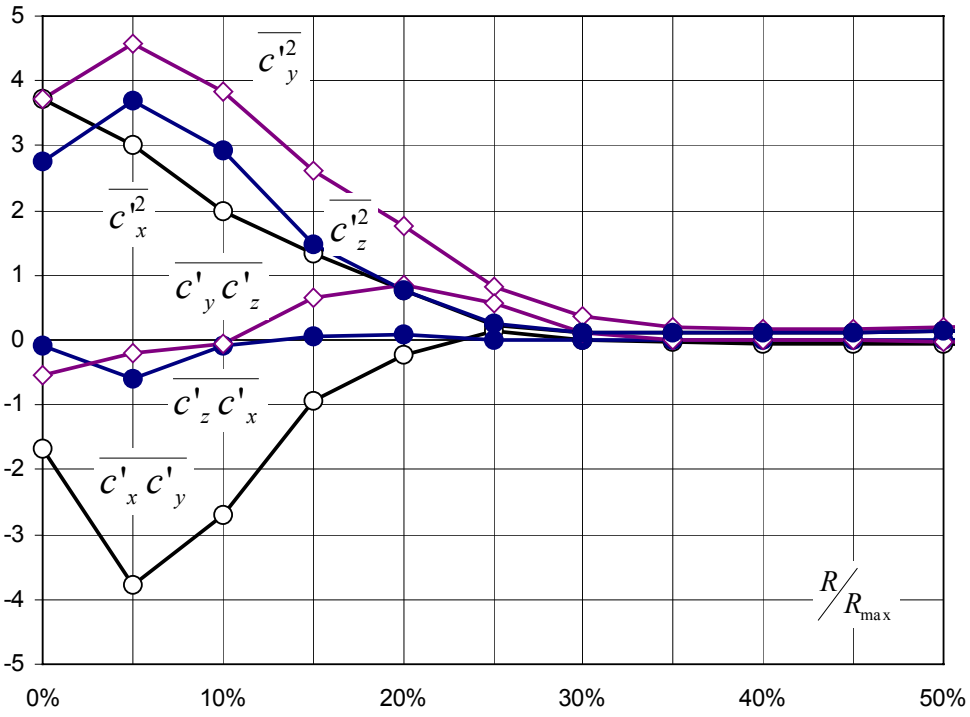

Figure 12 Radial distribution of the 6 components of the turbulent tensor at the core region of the inlet section of the draft tube, $\varphi = 0.350$.

FLOW ANALYSIS

The flow analysis in the draft tube is carried out with the help of CFX-TASCflow® version 2.9 (Ref. 15) which solves numerically the incompressible Reynolds-averaged Navier-Stokes equations with $k-\varepsilon$ turbulence modeling coupled with logarithmic wall functions to model the viscous near-wall layer. The computational procedure of this finite volume RANS solver is fully detailed by Mauri et al. (Ref. 16). It should be mentioned that the finite element RANS solver N3S® (Ref. 1) is also used within the FLINDT project, however in this paper only the flow analysis with CFX-TASCflow® is described.

As already mentioned, the steady inlet conditions are given by the experimental flow surveys at the inlet section of the draft tube for the operating points of interests, Table 2. To carried out the steady flow analysis, the 3 components of the velocity and the k and ε turbulent variables are needed at the inlet section, Figure 13.

Operating Point $\psi = 1.15$	**#1**	**#2**	**#3**
Q/Q_{bep}	92%	99%	111%

Table 2 Investigated Operating points

For this section, we could compare the flow velocity distribution given by both the 5 holes probe and the LDA measurements. The measurements show a very good agreement excepted for the radial component for which occurs a shift between the 2 types of measurements. This shift can be explained by an accuracy problem due to the very low values of the radial

component. Therefore this component is estimated by adjusting the offset of the curve in order to fulfill the radial symmetry.

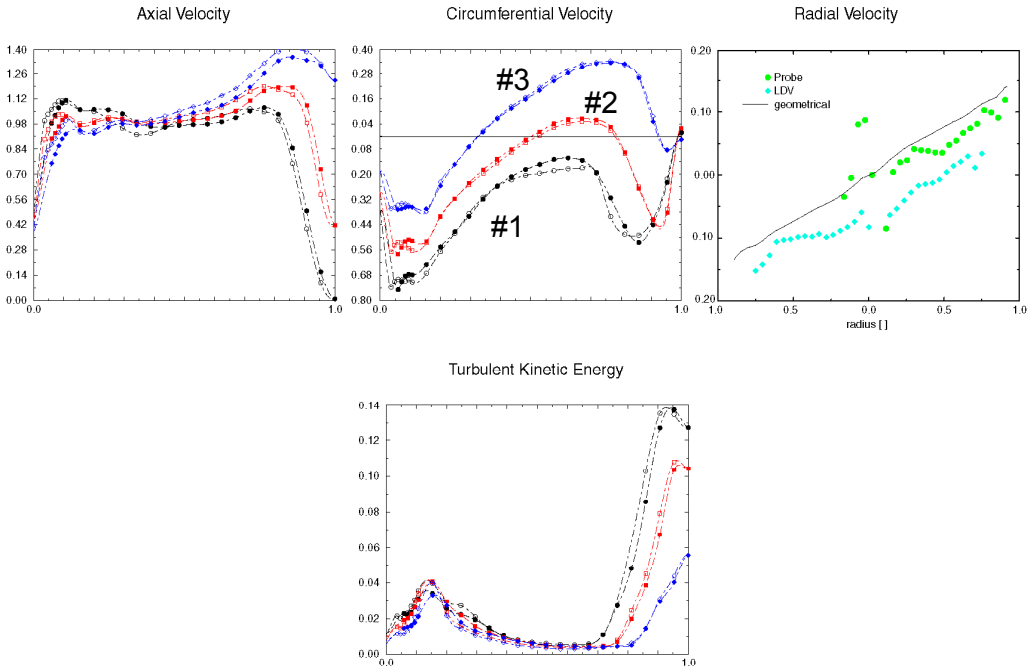

Figure 13 Radial distribution of the 3 velocity components and the turbulent specific kinetic energy at the inlet section of the draft tube for the 3 operating points of Table 2

The turbulent specific kinetic energy distribution is directly derived from the LDA measurement, however ε, the specific viscous dissipation energy, can only be estimated from a turbulent model of the turbulent viscosity. In the standard $k-\varepsilon$ model, it is assumed that $\varepsilon = k^{3/2}/l_t$. For the determination of ε from the measured turbulent kinetic energy, the turbulent length scale l_t defining the size of the largest eddies must be determined. This can be carried out according to the Prandl-Kolmogorov modeling of the turbulent viscosity, $\mu_t = \rho c_\mu l_t \sqrt{k}$, c_μ the constant of the $k-\varepsilon$ model. being assumed to remain unchanged.

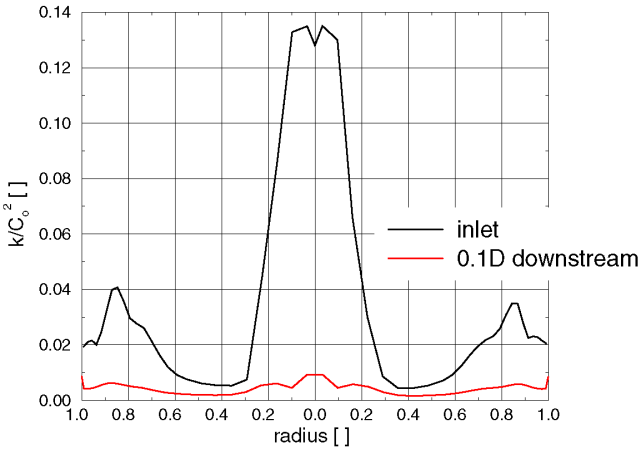

Figure 14 Stream wise evolution of the turbulent specific kinetic energy

Thus the turbulent viscosity can be evaluated from the LDA measurements by the relation.

$$-\overline{c'_i c'_j} = \frac{\mu_t}{\rho}\left(\frac{\partial C_i}{\partial x_j} + \frac{\partial C_j}{\partial x_i}\right)$$

The estimation shows that the length is nearly constant excepted in the central zone and near the wall. The corresponding value is about 2% of the runner diameter and thus of the same order of magnitude of the runner blades opening. However, the best numerical results with respect to the measurements are obtained with one order of magnitude smaller values, i.e. 0.2% of the runner diameter. The computational results show that the imposed turbulent kinetic energy profile with the important peak in the central zone is diffused in a very short distance, see Figure 14. Indeed if an uniform radial distribution of k is imposed, only negligible influence are observed on the computational results.

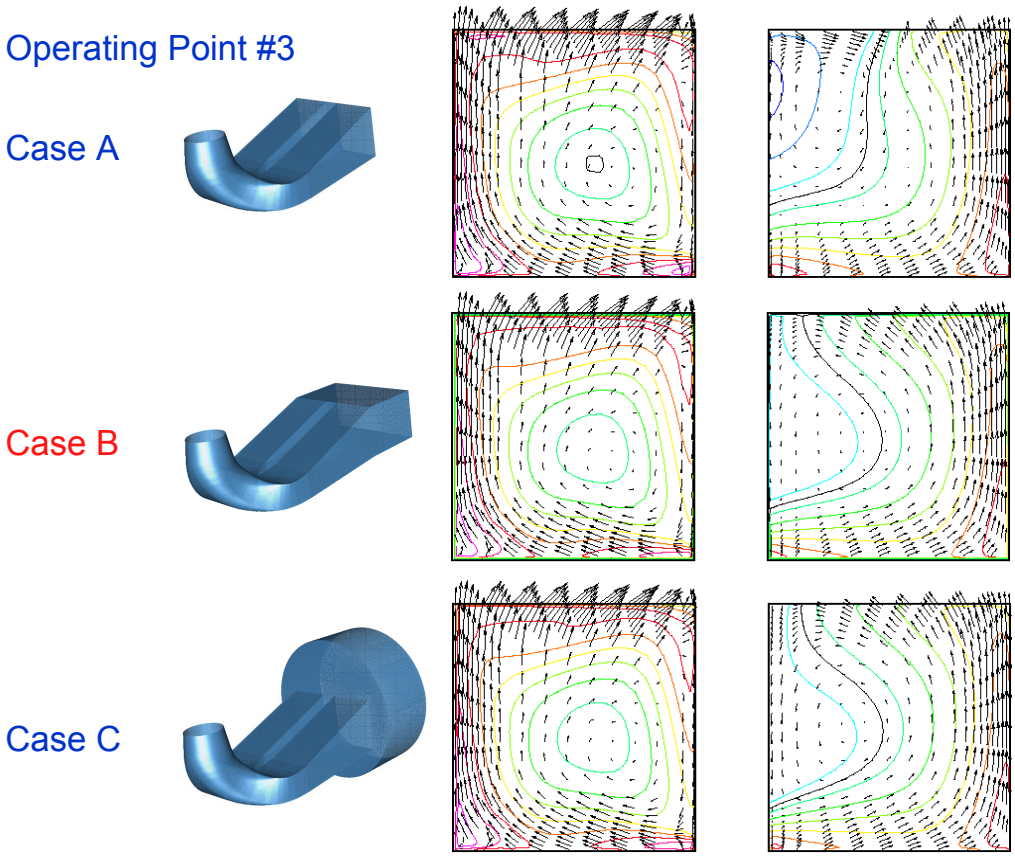

Figure 15 Influence of the downstream geometry on the flow velocity field at A_2, the outlet section of the draft tube, contour plot of the normal velocity component and tangential velocity vectors, operating point #3.

The numerical scheme of the CFD code used requires a special treatment for the boundary conditions depending if it is either an "inlet" or "outlet" boundary. In the case of the draft tube a back flow can take place at the outlet of 1 channel of the draft tube and, thus, influences the flow in the neighboring channel. Therefore, in that case the imposed outlet boundary condition would be no longer valid and moreover the exchange of information between the 2 channels would be impossible. To overcome this, a simple solution can be to add a volume at the outlet of the draft tube. Then, 3 different outlet configurations are investigated, Figure 15 :

- case A, only the draft tube geometry is computed with a zero stress condition at the outlet ;
- case B, a simple box is added downstream the draft tube ;

– case C, the test rig downstream tank is computed. Moreover, the existing settling grids in the tank are represented by using a porous region loss model.

The corresponding computation results show a negligible influence on the flow velocity field even for the expected worst case, operating point #3, for which a strong back flow in the right channel is observed. Thus, for the following flow analysis, only the case A is used as outlet boundary condition.

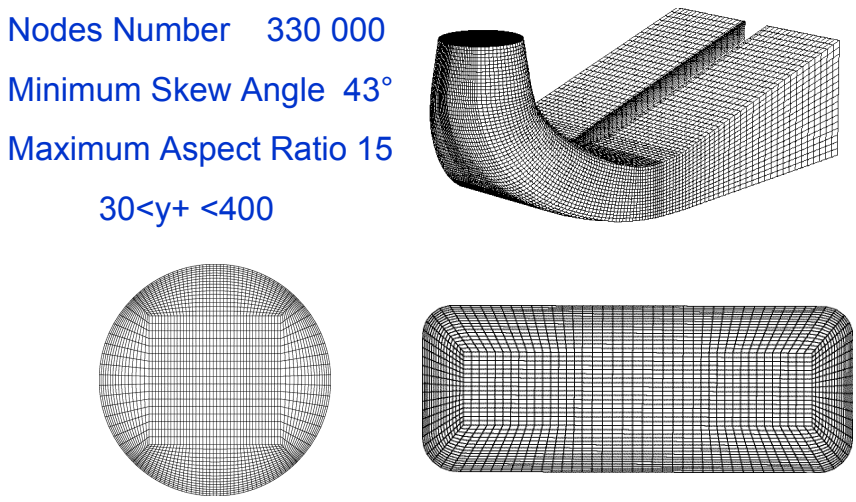

Figure 16 Structured multi block mesh, 330 000 nodes

The flow volume of the draft tube is discretized with a structured multi block mesh, see Figure 16. A butterfly topology with a C-shaped grid around the pier is used. The results of the computations performed for 3 sizes of mesh the operating point #3 are tested , Figure 17. The grid error estimation for the medium size mesh of 330 000 nodes is 4% . The medium size mesh is then used for the rest of the analysis.

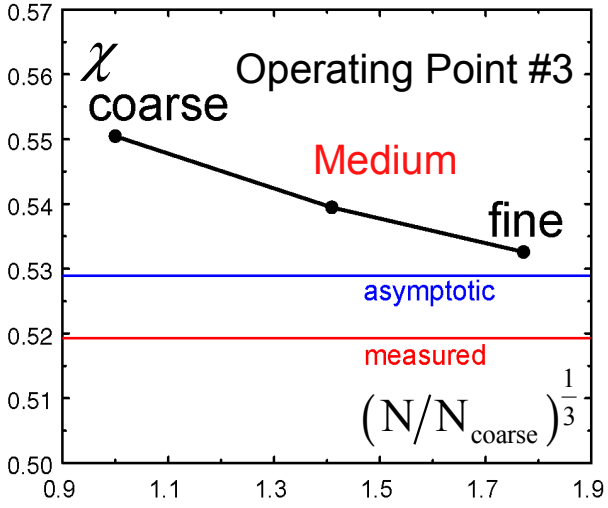

Figure 17 Influence of the mesh size on the pressure recovery coefficient, operating point #3, the medium size mesh corresponds to the mesh of Figure 16

For the purpose of the global validation of the flow analysis results, a total of 6 operating points are computed and compared to the pressure recovery coefficient. It can be observed a rather good agreement closed to the best efficiency discharge, however the discrepancy with

the experimental values are rather important, up to a maximum difference of 7% for a 3% averaged difference. However, it should be noticed that the break off is well captured.

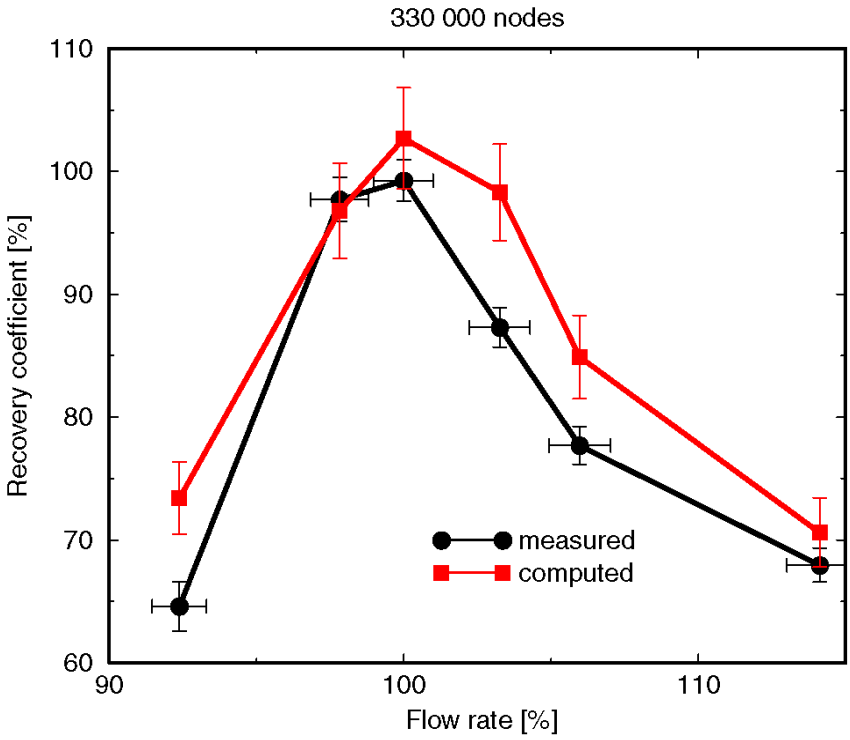

Figure 18 Comparisons of the computed pressure recovery coefficient with the experimental values, medium size mesh, $\psi = 1.15$.

The comparisons with the measurements in the section 1 at the inlet of the draft tube elbow, see Figure 19, show relatively important differences for all the velocity components; especially for operating point #1, where the swirl is stronger, despite the short distance from the inlet. The averaged difference values are 10% of the local mean velocity value and the maximum is as high as 50%. This could be explained by the known difficulties of the $k-\varepsilon$ model to correctly predict swirling flows. Another reason could be the influence of the unsteadiness that is not taken into account here.

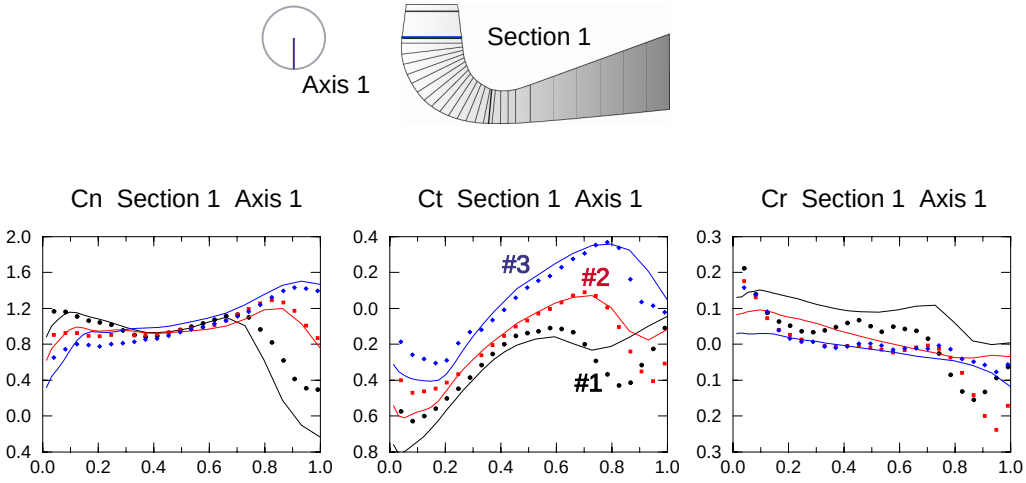

Figure 19 Comparisons of the radial distribution of the computed velocity components (solid lines) with the experimental values, medium size mesh, section 1, $\psi = 1.15$.

Owing to the number of flows surveys available, 7 axes, a more detailed comparisons can be carried out for this section for the operating point #1 (low discharge value) which experiences the largest discrepancies between computed and measured values. In this case, we also present Figure 20 the static pressure and the specific hydraulic energy of the flow. The agreement is good for all the variables excepted for the axial component c_n in the core region of high swirl which confirms the observation made for Figure 19.

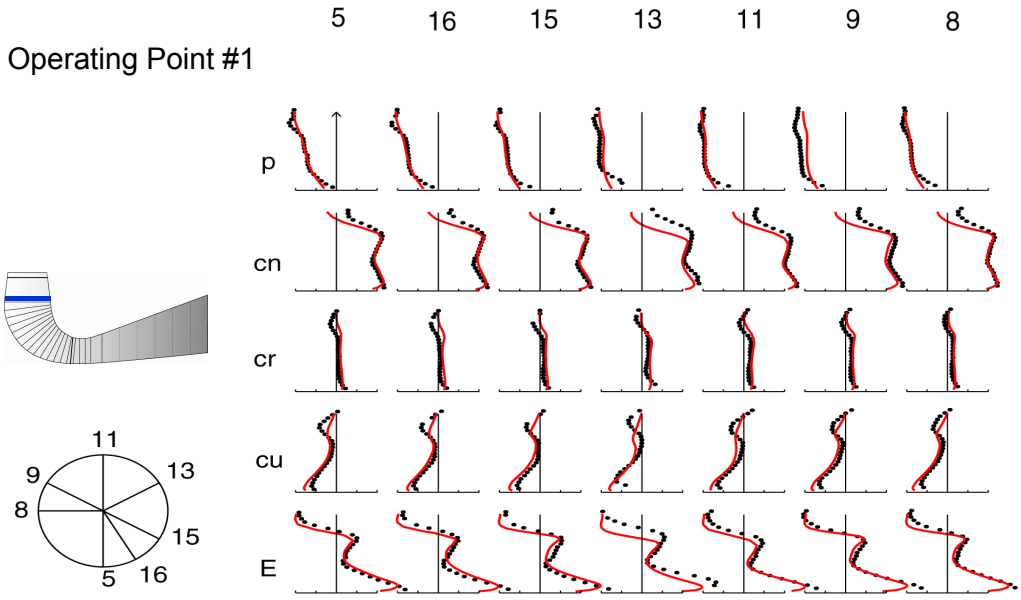

Figure 20 Comparisons of the radial distribution of the computed velocity components (solid lines) with the experimental values, section 1, operating point #1

Upstream to the pier, section 2, local important differences also take place but, globally, the evolution of the velocity is rather well predicted, see Figure 21. The averaged difference values ranges from 10% to 30% of the mean value of the velocity, the maximum difference values rising up to 50% in the right channel for the operating point #3. An estimation of the flow rate in the two channels, from nine measured vertical axes, shows a maximum difference of 10% with respect to the computation results.

CONCLUSION

An optimization of the draft tube can improve considerably the efficiency of low head hydroelectric power stations. Today CFD as design and analysis tool is applied routinely. An evaluation of the numerical prediction capability is therefore fundamental. The FLINDT Project intent to build up an experimental data base for the purpose of the validation of computational flow analysis of elbow draft tubes. The specific instrumentation of the draft tube with miniature pressure transducers, the flow surveys performed with both 5 holes pressure probes and LDA give the opportunity to compare the 3D steady Reynolds-averaged Navier-Stokes computations with the experimental data measured on the reduced scale model. Three operating points with different flow rates and a constant head are investigated. LDA measurements results are imposed as the inlet boundary condition. The influence of the inlet turbulence and the outlet boundary conditions are investigated and the role of the mesh is checked as well. Then, the flow analysis is carried out for different discharge coefficients at a constant specific energy coefficient. From an engineering point of view, the comparisons with the experimental values of the global quantities show a good agreement, in particular for the

the pressure recovery coefficient. However, the local analysis shows discrepancies results with the measurements, comparisons carried out at 2 sections, upstream of the elbow and downstream of the pier. These discrepancies are due to the $k-\varepsilon$ turbulent model which is diffusing in the region of high swirl flows and indicate the need for further turbulent modeling improvements. Therefore, at the end of the FLINDT project, there is not doubt that the built up experimental data will represent an invaluable set of knowledge for the understanding of the flow in an elbow draft tube.

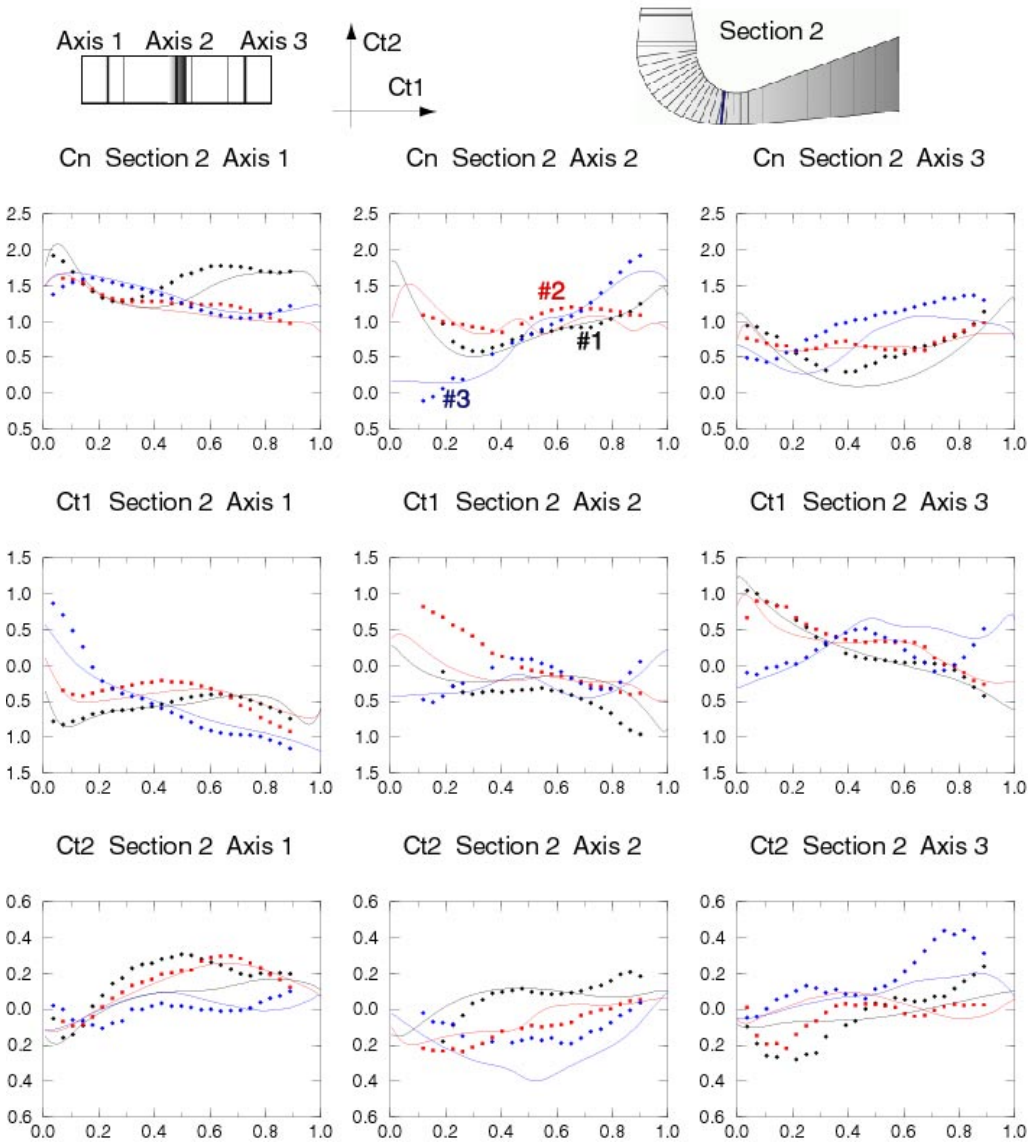

Figure 21 Comparisons of the axial distribution of the computed velocity components (solid lines) with the experimental values, medium size mesh, section 2, $\psi = 1.15$.

ACKOWLEDGEMENT

The study reported in this paper is part of the work carried out for the FLINDT Project whose participants are six of the major actors in the field of hydraulic machines. The partners are: The Swiss Federal Institute of Technology of Lausanne, Electricite de France, Alstom, General Electric Canada, Sulzer Hydro, Va Tech Voest Alpine MCE, Voith Hydro. The

project is also supported by the Swiss Federal Commission for Technology and Innovation (PSEL) and the German Ministry of Science and Technology (BMBF). SECAL has made available the turbine model. The author wish to thank G. Ciocan and J. Arpe for the LDA and the steady probe measurements, S. Mauri, J.-L. Kueny and F. Longatte for the flow analysis and J. Prénat for his help in the project management. The author is very grateful to the FLINDT Technical Committee for its involvement and constant support to the project. Finally the staff of the Laboratory for Hydraulic Machines should be thank for its support in the experimental and numerical work.

REFERENCES

Ref. 1 Vu, T. C., Shyy, W., 1988, "Viscous flow analysis for hydraulic turbine draft tubes", *Proceedings of 14th I.A.H.R. Symposium on Progress within large and high-specific energy units,* 20-23 June 1988, Trondheim, vol. 2, Session N, pp. 915-926.

Ref. 2 Tanabe., S., Ikegawa, M., Takagi, T., Sato, J., 1990, "Turbulent flow analysis in water turbine draft tube ", *Proceedings of 15th I.A.H.R. Symposium on Modern technology in hydraulic energy production,* 11-14 September 1990, Belgrade, vol. 1, Session G, Paper 12, 12 pages.

Ref. 3 Combes., J. F., Verry, A., Delorme, M., Philibert, R., Vanel J. M., 1990, "Numerical and experimental analysis of the flow inside an elbow draft tube ", *Proceedings of 15th I.A.H.R. Symposium on Modern technology in hydraulic energy production,* 11-14 September 1990, Belgrade, vol. 1, Session G, Paper 5, 12 pages.

Ref. 4 Rupprecht., A., 1990, "Numerical analysis of the flow in the elbow draft tube of a Kaplan Turbine", *Proceedings of 15th I.A.H.R. Symposium on Modern technology in hydraulic energy production,* 11-14 September 1990, Belgrade, vol. 1, Session G, Paper 6, 12 pages.

Ref. 5 Rupprecht., A., 1994, "Experimental and Numerical analysis of the three dimensional flow in elbow draft tubes", *Proceedings of 17th I.A.H.R. Symposium on Hydraulic Machinery and Cavitation,* 15-19 September 1994, Beijing, vol. 1, Session A, Paper A-5, pp. 83-94.

Ref. 6 Parkinson, E., Dupont, P. Hirschi, R., Huang, J., Avellan, F., 1994, "Comparison of flow computation results with experimental flow surveys in a Francis turbine", *Proceedings of 17th I.A.H.R. Symposium on Hydraulic Machinery and Cavitation,* 15-19 September 1994, Beijing, vol. 1, Session A, Paper A-2, pp. 45-57.

Ref. 7 Ventikos, Y., Sotiropoulos, F., Patel, V. C., 1996, "Modeling complex draft-tube flows using near wall turbulence closures.", in *Hydraulic Machines and Cavitation, Proceedings of 18th I.A.H.R. Symposium on Hydraulic Machinery and Cavitation*, Ed. Cabrera, Espert, Martinez, Kluwer Academic Publishers, Dordrecht, NL, pp. 140-149

Ref. 8 Keck H., Drtina P., Sick M., 1996, "Numerical hill chart prediction by means of CFD stage simulation for a complete Francis turbine", in *Hydraulic Machines and Cavitation, Proceedings of 18th I.A.H.R. Symposium on Hydraulic Machinery and*

Cavitation, Ed. Cabrera, Espert, Martinez, Kluwer Academic Publishers, Dordrecht, NL, pp. 170-179

Ref. 9 Nichtawitz, A., Abfalterer, J., 1990, "Model tests on various draft tube designs at high specific speed turbines". *Proceedings of 15th I.A.H.R. Symposium on Modern technology in hydraulic energy production,* 11-14 September 1990, Belgrade, vol. 1, Session G, Paper 4, 11 pages.

Ref. 10 EUREKA "A Euro-wide Network for Industrial R&D" http://www3.eureka.be/home/

Ref. 11 IEC 60193, 1999, *International standard : hydraulic turbines, storage pumps and pump-turbines. Model acceptance tests*, Geneva, 1999.

Ref. 12 Ciocan, G., Avellan, F., Kueny, J.-L., 2000, "Optical Measurement Techniques for Experimental Analysis of Hydraulic Turbines Rotor-Stator Interaction", *Proceedings of the ASME 2000 Fluids Engineering Division*, Summer Meeting, June 11-15, 2000, Boston, Paper FEDSM2000-11056, 7 pages.

Ref. 13 Avellan, F., Dupont, Ph., Farhat, M., Gindroz, B., Henry, P., Hussain, M., Parkinson, E., Santal., O., 1990, "Flow Survey and Blade Pressure Measurements in a Francis Turbine Model", *Proceedings of 15th I.A.H.R. Symposium on Modern technology in hydraulic energy production,* 11-14 September 1990, Belgrade, vol. 2, Session I, Paper I4, 14 pages.

Ref. 14 Avellan, F., Etter, S., Gummer, J. H., Seidel, U., 2000, "Dynamic pressure measurements on a model turbine runner and their use in preventing runner fatigue failure", *Proceedings of 20th I.A.H.R. Hydraulic Machinery and Systems,* 7-9 August 2000, Charlotte, vol. 1, Session DES, Paper DES-11, 12 pages.

Ref. 15 AEA Technology Engineering Software Limited, 1999, *CFX-TASC Flow Theory Documentation Version 2.9*, Waterloo, Ontario, Canada N2L 5Z4.

Ref. 16 Mauri, S., Kueny, J.-L., Avellan, F., 2000, "Numerical Prediction of the Flow in a Turbine Draft Tube, Influence of the Boundary Conditions", *Proceedings of the ASME 2000 Fluids Engineering Division*, Summer Meeting, June 11-15, 2000, Boston, Paper FEDSM2000-11056, 7 pages.